

## SIMULATION INVESTIGATION OF AN ACTIVE VIBRATION PROTECTION SYSTEM OF AN OPERATOR OF A HAND-HELD PERCUSSIVE TOOL

Z. B a s i s t a

Institute of Applied Mechanics  
Cracow University of Technology  
Kraków, Poland  
e-mail: zbas@mech.pk.edu.pl

In the paper a complex model of the system operator-tool-base (OTB) has been presented. The evaluation and choice of the correct vibration isolation system of the grip of hand-held percussive tools requires a proper model of the system OTB. In the OTB model adapted in the paper, the model of the man-operator describes not only the dynamical reaction of the operator hands to vibration but also the behaviour of the operator as a system which controls the tool operation. Using this model, the necessary criteria for the assessment of the working comfort are formulated. Simulation of the model OTB with the proposed nonlinear pneumatic active vibration isolation system was done applying the Matlab-Simulink. The influence of parameter values of the vibration isolation system on the assumed comfort criteria was analyzed. The results obtained have been graphically presented.

**Key words:** hand-held percussive tools, active vibration isolation, man-machine systems, human-operator.

### 1. INTRODUCTION

One way of reducing the harmful vibration acting on the hands of the human operator is to isolate the tool handle by means of a vibration isolation system. The use of a vibration isolation system increases the work comfort as a result of lower handle vibration levels, but at the same time it can provoke a feeling of discomfort of the operator who may find it to be more difficult to operate and control the tool. This latter effect should be taken into account when designing a vibration isolation system and a broader approach is needed which would take into account both comfort factors mentioned above.

The basis of building the simulation model used in the present paper is the block diagram of the system operator-tool-base shown in Fig. 1 [1–3]. The system operator-tool-base (OTB) is treated here as a man-machine system [4] and the operation of the tool as a manual control problem. The controlled variable of the problem is the efficiency of the chiselling process  $v$  (the rate at which the

chisel penetrates into the base). In order to achieve the assumed efficiency  $v_z$ , the operator acts on the handle with an appropriate pressure force  $F$  which in the considered block diagram is the only control function realized by the operator. Using the block diagram of Fig. 1 together with appropriate models of the human operator, the vibration isolation system and the tool and the base, the model of the overall system operator-tool-base has been developed in Simulink. For such a model a study has been done with a view to analysing the influence of the proposed vibration isolation system on the two comfort criteria used.

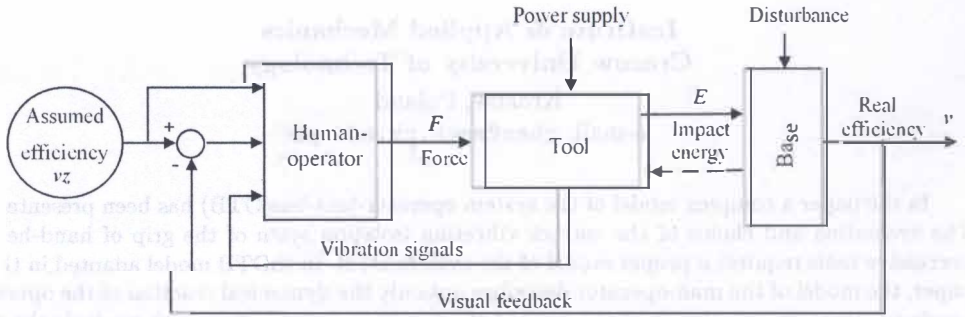


FIG. 1. Block diagram of the operator-tool-base system.

## 2. MODEL OF THE HUMAN OPERATOR

The human operator who acts as a regulator in a man-machine system has been modelled in various ways [1]. Most frequently these models have been used to simulate pilot's reaction in controlling the airplane or the behaviour of car drivers. At present no experimentally verified models exist which can be used in the system man-hand-operated tool. Hence, one is forced to make use of the above mentioned models, assuming that the behaviour of a human operator of a hand tool is similar to that of a vehicle driver. The adopted simulation model of the human operator is shown in Fig. 2. Its principal part is based on a driver model [5], supplemented by the model proposed by Miwa (as described in [6], look Fig. 3, Formula (2.1)) which represents the passive reaction force brought about by the handle vibration. As the input of the system one has:  $a_x$  – the acceleration of the handle vibration,  $v_z$  – the assumed chiselling efficiency,  $e = v_z - v$  – control error,  $x$  – displacement of the handle. The output signal  $F$  is the overall force acting on the handle, which consists of a slowly-varying control force and a fast dynamical reaction of the hands. The quantity  $u_m$  models the proprioceptive signal in the neuromuscular system. This signal has been used to define the criterion index describing the second of the comfort factors described above.

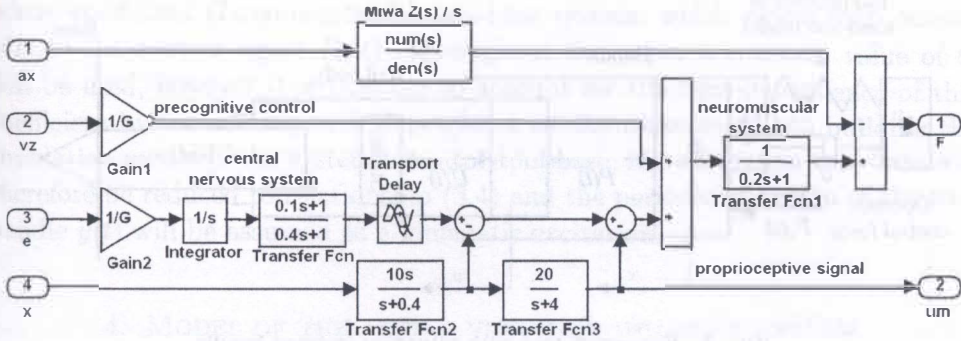


FIG. 2. Simulation model of the human-operator.

The model shown realizes the compensation control which minimizes the control error and the so-called precognitive control (the control which utilizes earlier experience). The constant parameters of individual blocks have been chosen from the range specified in the literature [4, 5]. Some of the parameters can undergo changes during the adaptation process of the human operator, but this problem is not considered in the present paper. The dynamical reaction of operator's hands on the handle vibrations is described by the block with transmittance  $Z(s)/s$ , where  $Z(s)$  is the input impedance of the mechanical model described by Miwa [6]

$$(2.1) \quad Z(s) = s \frac{m_1 m_2 s^2 + \alpha(m_1 + m_2)s + k(m_1 + m_2)}{m_2 s^2 + \alpha s + k},$$

where:  $m_1 = 0.1$  [kg],  $m_2 = 0.8$  [kg],  $\alpha = 250$  [Ns/m],  $k = 130 \cdot 10^3$  [N/m].

### 3. MODEL OF THE TOOL-BASE SYSTEM

The percussive tool (pneumatic hammer, riveter, demolition hammer etc.) shown in Fig. 3 can be described as a transducer which changes the energy of the source into the vibro-impact process [7]. In order to transmit the energy of the source to the base and ensure the correct operation of the tool, it is necessary to exercise a required pressure force on the tool body, from within a range specified by its minimum and maximum values. The correct and most efficient operation of the tool takes place at the condition when there is one impact of the striker on the tool during each work cycle with period  $T$ . If a vibration isolation system is used, the operator who controls the tool acts with a pressure force  $F_0(t)$  on the handle. The force with which the vibration isolation system acts on the tool body is equal to  $P(t)$ . This force consists of a fast periodic component  $P_1(t)$  related

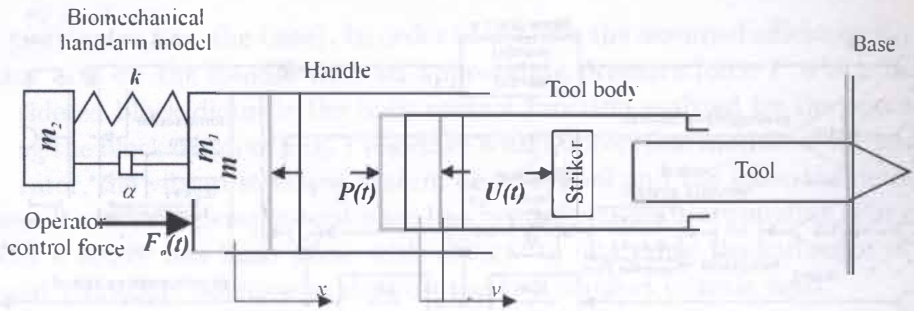


FIG. 3. Percussive tool with vibration isolated handle.

to the vibro-impact process and a slowly-varying component  $P_0(t)$ , calculated as the following average:

$$(3.1) \quad P_0(t) = \frac{1}{T} \int_{t-T}^t P(\tau) d\tau.$$

The force  $P_0(t)$  results from the action of the slowly-varying component of the operator force on the handle  $F_0(t)$ , which is the main tool operation control function. BABITSKY [7] has shown, that a percussive tool can be described as a discrete modulator, which changes the slowly-varying pressure force  $P_0(t)$  acting on the tool body to a modulated sequence  $I(nT)$  of the striker pulses on the tool:

$$(3.2) \quad I(nT) \cong P_0(nT)T \sum_n \delta(t - nT),$$

where:  $\delta(t)$  – the Dirac delta function,  $n$  – number of an impact.

The efficiency of the chiselling process defined as  $v_n = b_n f$ , where  $b_n$  is the penetration of the tool into the base during the  $n$ -th impact and  $f = 1/T$  – the frequency of impacts, is expressed after reference [7] in the form of the following relationship:

$$(3.3) \quad v_n = G_n P_0(nT).$$

The coefficient  $G_n$  depends on the tool parameters and on the elastic-plastic properties of the base. Using the above developments, the process of embedding of the tool into the base is approximated by a continuous function, by reducing the relation (3.3) to the form:

$$(3.4) \quad v(t) = G P_0(t),$$

where coefficient  $G$  represents the tool-base system, which reacts with output  $v(t)$  to the control signal  $P_0(t)$ . Throughout the paper a constant value of  $G$  will be used, however it is possible to account for the time-dependence of this coefficient by considering such dependence as disturbances. When building the simulation model of the system operator-tool-base, the subsystem tool-base will therefore be reduced to relationship (3.4) and the periodic vibration of the tool handle  $y(t)$  will be assumed as a kinematic excitation.

#### 4. MODEL OF THE ACTIVE VIBRATION ISOLATION SYSTEM

The analysed vibration isolation system is shown in Fig. 4. The schematic drawing shown in this figure presents an idea of a design applicable to pneumatic percussive tools. The main elements of the system have been shown. The pneumatic chamber of variable volume  $V$  and pressure  $p$  isolates the handle from the tool body. The handle 1 is connected to cylinder 2 (the pneumatic chamber). Piston 3 connects to the tool handle. The inlet and outlet orifices 4 are opened and closed by the cylinder and piston edge during the relative displacement of the handle with respect to the handle. Compressed air with the pressure  $p_s$  supplied from an outlet of the compressed air network is also used for the operation of the vibration isolation system. The function of the additional spring 5 is to provide the initial tension and ensure that the system returns to its end position after the air supply is switched off. The limiters of motion (buffers) 6 are used in order to restrain relative displacements. Since the piston is connected to the tool body and is considered its part and the cylinder adds to the mass of the handle, the vibration isolation system will be treated as massless. The overall

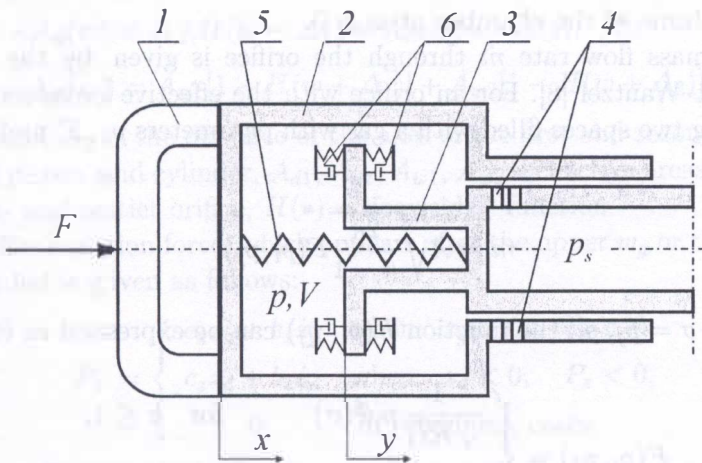


FIG. 4. Schematic drawing of an active vibration isolation system.

force  $P$  with which the vibration isolation system acts on the tool handle and body results from the force due to the variable pressure in the chamber, the resistance force of the piston moving inside the cylinder, the force in the additional spring and the reaction of the limiters of relative displacement acting at the end positions. The overall force generated by the vibration isolation system can thus be given as the following sum:

$$(4.1) \quad P = (p - p_a)S + b\dot{w} + F_t \text{sign}(\dot{w}) + P_w + c_s w + P_z,$$

where:  $w = x - y$  - is the relative displacement of the handle with respect to the tool body,  $p$  - absolute pressure inside the chamber,  $p_a$  - atmospheric pressure,  $S$  - piston area,  $b$  - coefficient of viscous resistance of piston inside cylinder,  $F_t$  - force of dry friction,  $P_w$  - pre-tension of additional spring,  $c_s$  - stiffness of additional spring,  $P_z$  - reaction of the buffers.

Assuming that the change in the pneumatic chamber is adiabatic and applying the first law of thermodynamics, the following differential equation can be obtained [8] which describes the pressure change inside the chamber:

$$(4.2) \quad \dot{p}V + \kappa p \dot{V} = \kappa R(\dot{m}_d T_s - \dot{m}_w T).$$

In Eq. (4.2)  $\kappa = 1.4$  is the adiabatic exponent,  $R = 287$  [Nm/kg °K] - gas constant,  $\dot{m}_d$  and  $\dot{m}_w$  - air mass flow rates through the inlet and outlet orifices,  $T_s$  - supply air temperature,  $T$  - air temperature inside the chamber. The variable volume  $V$  of the chamber is a function of relative displacement:

$$(4.3) \quad V = V_0 - Sw,$$

where  $V_0$  - volume of the chamber at  $w = 0$ .

The air mass flow rate  $\dot{m}$  through the orifice is given by the formula of Saint-Venant-Wantzel [8]. For an orifice with the effective cross-sectional area  $A$ , connecting two spaces filled with a gas with parameters  $p_i$ ,  $T_i$  and  $p_j$ ,  $T_j$ , one has:

$$(4.4) \quad \dot{m} = A \sqrt{\frac{2\kappa}{\kappa - 1}} F(p_i, p_j).$$

Denoting  $\sigma = p_j/p_i$ , the function  $F(p_i, p_j)$  can be expressed as follows:

$$(4.5) \quad F(p_i, p_j) = \begin{cases} \frac{1}{\sqrt{RT_i}} p_i \Phi(\sigma) & \text{for } \sigma \leq 1, \\ -\frac{1}{\sqrt{RT_j}} p_j \Phi(1/\sigma) & \text{for } \sigma > 1, \end{cases}$$

where:

$$(4.6) \quad \Phi(\sigma) = \begin{cases} \sqrt{\sigma^{2/\kappa} - \sigma^{\kappa+1/\kappa}} & \text{for } \sigma_{\text{cr}} < \sigma < 1, \\ \sqrt{\sigma_{\text{cr}}^{2/\kappa} - \sigma_{\text{cr}}^{\kappa+1/\kappa}} & \text{for } \sigma \leq \sigma_{\text{cr}}. \end{cases}$$

The critical value of the pressure ratio

$$(4.7) \quad \sigma = \left( \frac{2}{\kappa + 1} \right)^{\kappa/(\kappa-1)} = 0.5282$$

is the limit dividing the subcritical and supercritical flow regions. For  $F(p_i, p_j) > 0$  the gas flows from the  $i$ -th space to the  $j$ -th, whereas in the case of  $F(p_i, p_j) < 0$  the direction of the flow is reversed. Applying the above relationships to calculate  $\dot{m}_d$  and  $\dot{m}_w$ , using the assumption  $T = T_s$  and defining the function:

$$(4.8) \quad \Psi(p_i, p_j) = \begin{cases} p_i \Phi(\sigma) & \text{for } \sigma \leq 1, \\ -p_j \Phi(1/\sigma) & \text{for } \sigma > 1. \end{cases}$$

Equation (4.2) can be reduced to the form:

$$(4.9) \quad \dot{p}V + \kappa p \dot{V} = \kappa \sqrt{\frac{2\kappa RT_s}{\kappa - 1}} [A_d(w) \Psi(p_s, p) - A_w(w) \Psi(p, p_a)].$$

The effective cross-sectional areas  $A_d(w)$  and  $A_w(w)$  of the inlet and outlet orifices, respectively, are functions of the relative displacement  $w$ . In the present paper we consider the case when there are two inlet- and two outlet orifices of small diameters, situated at the same distance from the edge of the piston and cylinder (see Fig. 2), so that the above functions can be written in the following simple form:

$$(4.10) \quad \begin{aligned} A_d(w) &= A_{d1} H(w - \Delta_1) + A_{d2} H(w - \Delta_2), \\ A_w(w) &= A_{w1} [1 - H(w + \Delta_1)] + A_{w2} [1 - H(w + \Delta_2)], \end{aligned}$$

where:  $\Delta_1$  and  $\Delta_2$  - the distance of the axes of the first and second orifice from the edge of piston and cylinder,  $A_{d1}$ ,  $A_{d2}$ ,  $A_{w1}$ ,  $A_{w2}$  - effective areas, respectively of the inlet- and outlet orifice,  $H(\bullet)$  - Heaviside's function.

The buffer reaction force, which appears after the upper  $w_g$  or the lower limit  $w_d$  is exceeded is given as follows:

$$(4.11) \quad P_z = \begin{cases} c_z z_g + b_z \dot{z}_g & \text{when } z_g > 0, \quad P_z > 0, \\ c_z z_d + b_z \dot{z}_d & \text{when } z_d < 0, \quad P_z < 0, \\ 0 & \text{in remaining cases,} \end{cases}$$

where:  $c_z$  - stiffness of the buffer,  $b_z$  - viscous coefficient,  $z_g = w - w_g$ ,  $z_d = w - w_d$  - deformation of buffers.

## 5. SIMULATION MODEL OF THE SYSTEM OPERATOR-TOOL-BASE

Figure 5 illustrates a schematic drawing of the system used in the simulation studies. The system consists of three main subsystems: human operator, vibration isolation system and the tool-base system.

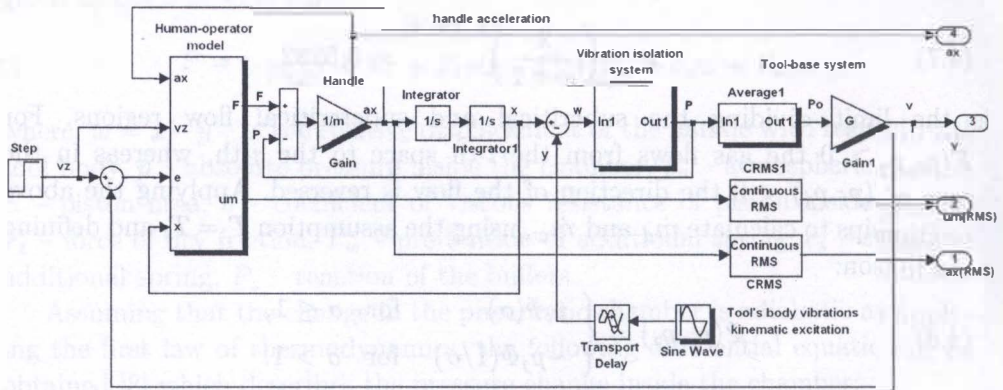


FIG. 5. Simulation model of the system operator-tool-base.

The handle is represented as an amplifier element with the gain equal to the reciprocal of the handle mass  $1/m$ . The model of the human operator has been described above. The vibration isolation system is represented by a block diagram (not shown) prepared in Simulink based on expression (4.1), equation (4.9) and relations (4.3)–(4.8), (4.10), (4.11). The tool-base system has been reduced according to (3.4) to a constant multiplier  $G$  with a prescribed value. The slowly-varying component  $P_0(t)$  of the interaction force of the vibration isolation system on the tool body has been obtained by passing the signal  $P(t)$  through a built averaging block (Average), which according to Eq. (3.1) averages the input signal in a moving time window with a set averaging time. At the input of the whole system one applies a test signal in the form of a step function. The vibration of the tool body has been treated as the prescribed kinematic excitation given by a harmonic function with frequency equal to the principal frequency of the tool operation. The main output quantity is the chiselling efficiency  $v$ . For reasons of analysis one also outputs: the handle acceleration  $a_x$ , rms acceleration  $a_x$  RMS and the rms value of the signal  $u_m$  RMS.

## 6. COMFORT INDICES

The operation of a percussive tool is as a rule characterized by a series of continuous operation cycles of several seconds' duration. Each such period starts

with an almost simultaneous switching on of the air supply and the application of a given pressure force to the handle. The operator can correct this force during operation by observing the process and the behaviour of the tool. As a result, the vibration isolation system operates mostly in transient states. The sudden application of the pressure force by the operator at the time when the tool is switched on and the subsequent possible necessity of changing this force during the operation cycle, causes substantial displacements of the handle relative to the tool body. These displacements, registered by the receptors in the operator's neuromuscular system [4], do not reflect the real embedding of the tool into the base which is observed visually. As a result, the operator has a sense of discomfort, caused by the deterioration of what is called the tool handling qualities. Therefore, apart from the vibrational comfort index defined as the vibration reduction ratio

$$(6.1) \quad W_1 = \frac{a_{y\text{RMS}}}{a_{x\text{RMS}}},$$

where  $a_{y\text{RMS}}$  and  $a_{x\text{RMS}}$  are the rms values of the vibration of the tool body and handle, respectively, we introduce another index in the form

$$(6.2) \quad W_2 = \frac{P_{\text{nom}}}{u_{m\text{RMS}}},$$

where  $P_{\text{nom}}$  is the nominal pressure force of the given tool (e.g. defined as the average value in the range of regular operation) and  $u_{m\text{RMS}}$  is the rms value of the proprioceptive feedback signal (see Fig. 2). This approach is consistent with [5] where the value  $u_{m\text{RMS}}$  is considered as a measure of the operator's workload during the control process. The rms values used by both comfort indices are calculated in the time interval corresponding to one cycle of continuous operation, and can be the basis of evaluating the quality of the vibration isolation system. An efficient vibration isolation system should ensure high enough values of both indices.

## 7. SIMULATION STUDIES

The simulation studies of the OTB system have been performed for a test input signal in the form  $v_z = 0.015H(t)$  [m/s], where  $H(t)$  denotes Heaviside's function. The tool-base system is characterized by the coefficient  $G = 10^{-4}$  [m/Ns]. This means (see (3.4)) that the ideal pressure force that the operator tries to achieve is a step function of value 150 [N]. The initial state of the vibration isolation system is given by:  $w(0) = (c_z w_d - P_w)/(c_s + c_z)$ ,  $p(0) = p_a$ . The simulation time corresponding to one cycle of continuous operation is equal to 10 [s]. The tool body vibration  $y(t)$  has been assumed in the form of a harmonic function with amplitude  $y_0 = 0.003$  [m] and frequency  $f = 30$  [Hz]. The

rms acceleration value is thus equal to  $a_{yRMS} = 75.37 \text{ [m/s}^2\text{]}$ . It has been further assumed that  $P_{nom} = 100 \text{ [N]}$ .

The vibration isolation system together with the handle is characterized by several parameters. The following values of constant parameters have been assumed:  $m = 1 \text{ [kg]}$  – mass of the handle,  $D = 0.03 \text{ [m]}$  – diameter of the bearing,  $\Delta_1 = 0.005 \text{ [m]}$ ,  $\Delta_2 = 0.015 \text{ [m]}$ ,  $w_g = 0.03 \text{ [m]}$ ,  $w_d = -0.03 \text{ [m]}$ ,  $c_s = 100 \text{ [N/m]}$ ,  $P_w = 10 \text{ [N]}$ ,  $c_z = 10^4 \text{ [N/m]}$ ,  $b_z = 100 \text{ [Ns/m]}$ . The variable parameters include: volume  $V_0$  of the pneumatic chamber in the middle position ( $w = 0$ ) of the vibration isolation system, effective areas of the inlet- ( $A_{d1}$ ,  $A_{d2}$ ) and outlet orifices ( $A_{w1}$ ,  $A_{w2}$ ) and viscous coefficient  $b$  of the piston moving inside the cylinder and the force of dry friction  $F_t$ . For the assumed values of the supply air pressure  $p_s = 6 \cdot 10^5 \text{ [N/m}^2\text{]}$  and atmospheric pressure  $p_a = 10^5 \text{ [N/m}^2\text{]}$  one can calculate the absolute pressure inside the chamber  $p_{nom}$  corresponding to the nominal pressure force  $P_{nom}$ :  $p_{nom} = P_{nom}/S + p_a = 2.4147 \cdot 10^5 \text{ [N/m}^2\text{]}$ , where  $S = \pi D^2/4 = 7.0686 \cdot 10^{-4} \text{ [m}^2\text{]}$  is the piston area. In order to ensure the symmetry of the control characteristic in the vibration isolation system it has been assumed that the following relations holds between the areas of the inlet and outlet orifices:

$$(7.1) \quad \frac{A_{d1}}{\Delta_1} \Psi(p_s, p_{nom}) = \frac{A_{d2}}{\Delta_2} \Psi(p_s, p_{nom}) = \frac{A_{w1}}{\Delta_1} \Psi(p_{nom}, p_a) \\ = \frac{A_{w2}}{\Delta_2} \Psi(p_{nom}, p_a) = q.$$

Thanks to this assumption, the number of variable parameters is limited to the damping coefficient  $b$ , friction force  $F_t$  and two parameters characterizing the vibration isolation system, which are defined as follows:

$$(7.2) \quad c = \frac{\kappa S^2 p_{nom}}{V_0} \quad \lambda = \kappa \sqrt{\frac{2\kappa RT_s}{\kappa - 1}} \frac{S}{V_0} q.$$

Parameter  $c$  can be interpreted as the stiffness of the pneumatic chamber corresponding to position  $w = 0$  and the pressure in the chamber  $p = p_{nom}$ . Parameter  $\lambda$  is the gain coefficient in the system controlling the air inlet and outlet to and from the pneumatic chamber. The latter parameter reflects the degree of “activity” of the vibration isolation system. In the case when  $\lambda = 0$  the pneumatic chamber is fully closed and the vibration isolation system is a passive one. By repeating many times in a loop the simulation process for different values of variable parameters, the plots have been obtained illustrating the influence of these parameters on the comfort indices defined above.

The plots shown in Figs. 6 and 7 illustrate the influence of the parameter  $\lambda \text{ [N/ms]}$  on the values of  $W_1$  and  $W_2$ , for the prescribed stiffness  $c = 2 \cdot 10^3 \text{ [N/m]}$

and different values of the viscous damping coefficient  $b$  (dry friction force  $F_t = 0$ ). The curves correspond to the values  $b = 10, 20, 30, 40$  [Ns/m], respectively. Figure 6 considers a vibration isolation system where no buffers limiting the relative displacements have been used, Fig. 7 considers the case with buffers. Figure 8 shows similar plots for the case without buffers for  $b = 0$  for different values of the dry friction force  $F_t$ . The corresponding curves have been obtained for values  $F_t = 5, 10, 15, 20$  [N]. Figure 9 illustrates the influence of the stiffness of the vibration isolation system  $c$  [N/m] on the values of indices  $W_1$  and  $W_2$  for different values  $\lambda = 0, 0.5 \cdot 10^4, 1.5 \cdot 10^4, 2 \cdot 10^4$  [N/ms] and set values  $b = 20$  [Ns/m],  $F_t = 0$ .

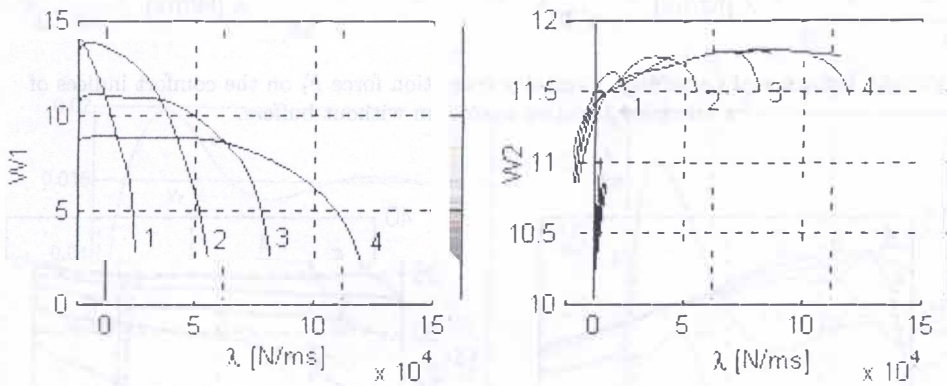


FIG. 6. Influence of parameter  $\lambda$  and coefficient  $b$  on the comfort indices of a vibration isolation system without buffers.

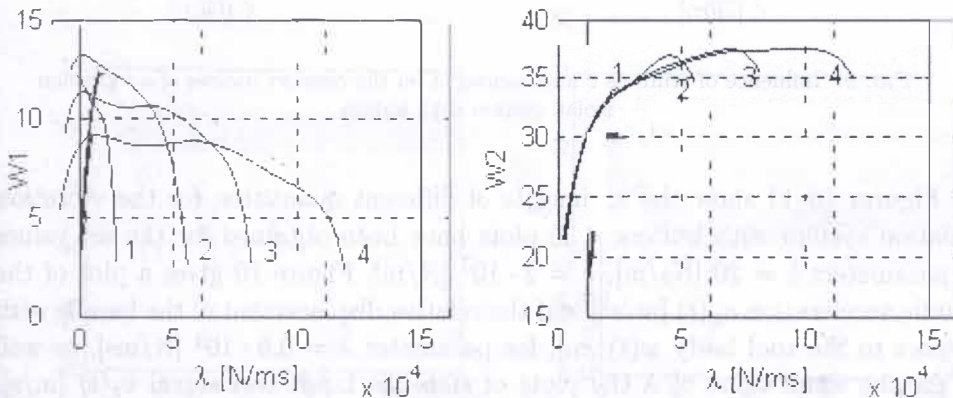


FIG. 7. Influence of parameter  $\lambda$  and coefficient  $b$  on the comfort indices of a vibration isolation system with buffers.

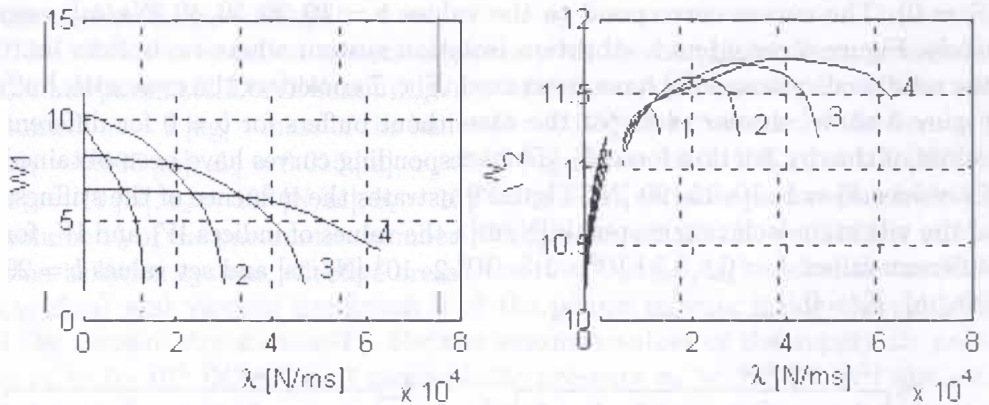


FIG. 8. Influence of parameter  $\lambda$  and dry friction force  $F_i$  on the comfort indices of a vibration isolation system without buffers.

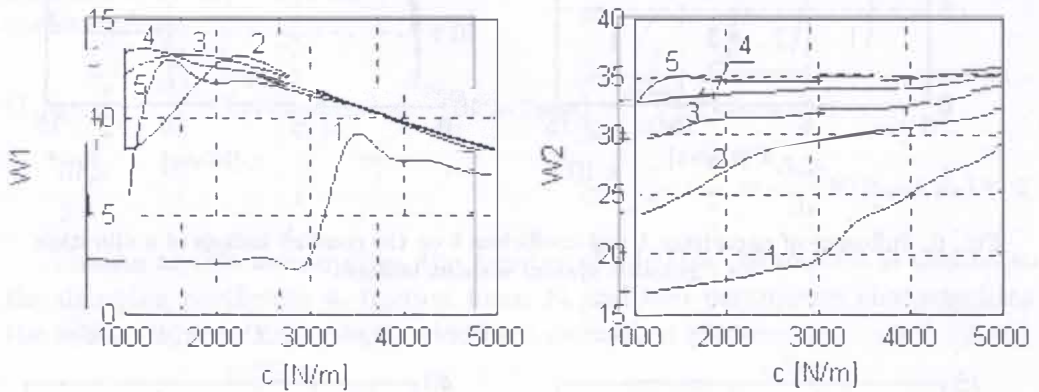


FIG. 9. Influence of stiffness  $c$  and parameter  $\lambda$  on the comfort indices of a vibration isolation system with buffers.

Figures 10–11 show the time plots of different quantities, for the vibration isolation system with buffers. The plots have been obtained for the set values of parameters  $b = 20$  [Ns/m],  $c = 2 \cdot 10^3$  [N/m]. Figure 10 gives a plot of the handle acceleration  $a_x(t)$  [m/s<sup>2</sup>] and the relative displacement of the handle with respect to the tool body  $w(t)$  [m], for parameter  $\lambda = 0.5 \cdot 10^4$  [N/ms], as well as for the same value of  $\lambda$  the plots of step-like input test signal  $v_z(t)$  [m/s], the output signal (the achieved chiselling efficiency)  $v(t)$  [m/s] and the time-dependence of  $u_m(t)$ . Figure 11 shows plots of  $a_x(t)$  and  $w(t)$  obtained for  $\lambda = 2 \cdot 10^4$  [N/ms].

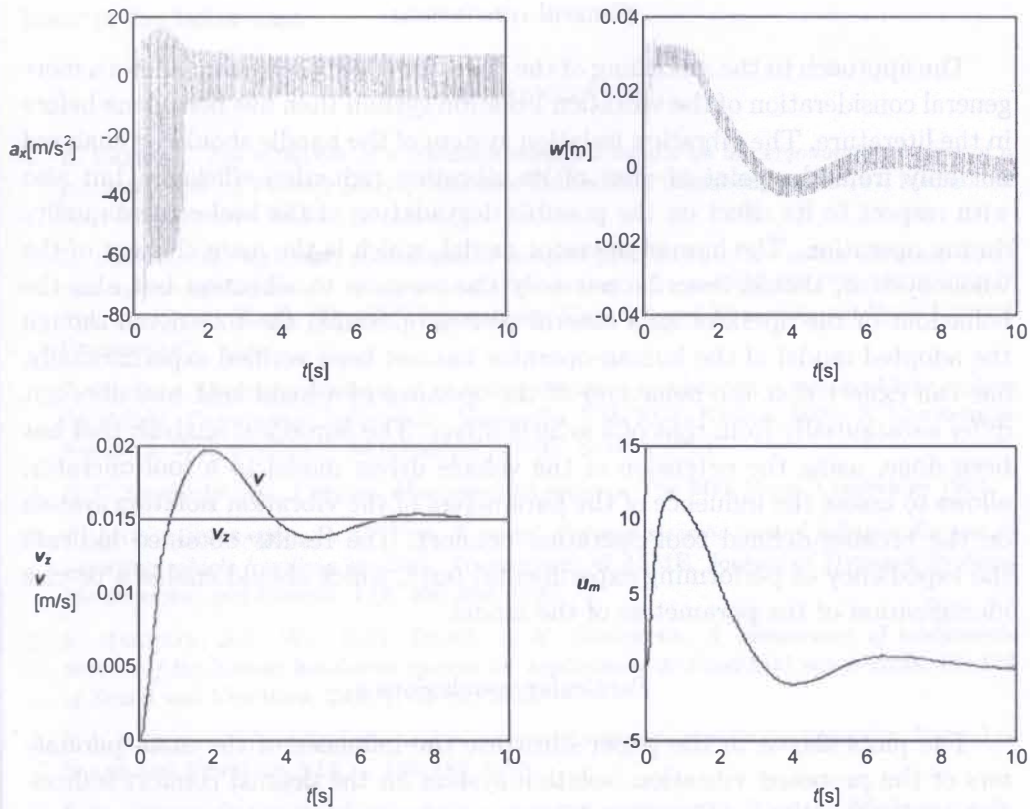


FIG. 10. Time histories of  $a_x(t)$ ,  $w(t)$ ,  $v_z(t)$ ,  $v(t)$ ,  $u_m(t)$  for  $\lambda = 0.5 \cdot 10^4$  [N/ms].

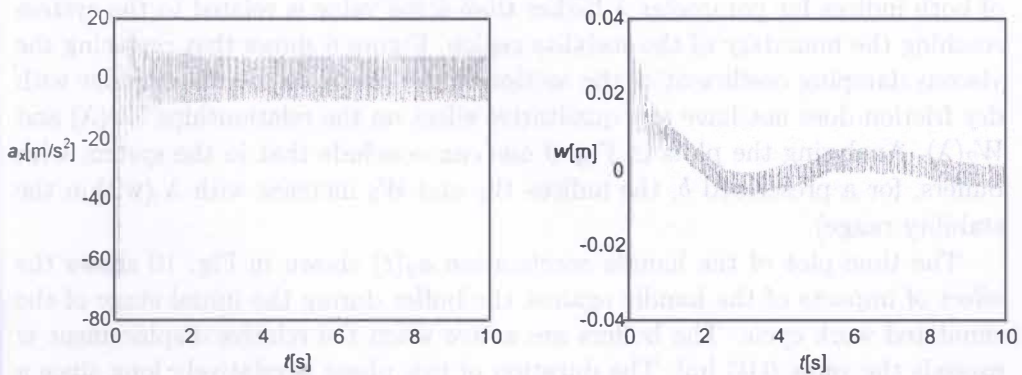


FIG. 11. Time histories of  $a_x(t)$  and  $w(t)$  for  $\lambda = 2 \cdot 10^4$  [N/ms].

## 8. CONCLUSIONS

### *General conclusions*

The approach to the modelling of the operator-tool-base system allows a more general consideration of the vibration isolation system than has been done before in the literature. The vibration isolation system of the handle should be analysed not only from the point of view of its vibration reduction efficiency, but also with respect to its effect on the possible degradation of the tool control quality during operation. The human-operator model, which is the main element of the whole system, should describe not only the reaction to vibration but also the behaviour of the operator as a control system operating the tool. Even though the adopted model of the human-operator has not been verified experimentally, one can expect that the behaviour of the operator of a hand-held tool does not differ substantially from that of a vehicle driver. The numerical analysis that has been done, using the extension of the vehicle driver model to a tool operator, allows to assess the influence of the parameters of the vibration isolation system on the broader-defined tool operation comfort. The results obtained indicate the expediency of performing experimental tests, which should enable a precise identification of the parameters of the model.

### *Particular conclusions*

The plots shown in the paper illustrate the influence of the main parameters of the proposed vibration isolation system on the defined comfort indices. Comparing the plots of Figs. 6 and 7 one can observe that only an active system ( $\lambda > 0$ ) can ensure that both indices  $W_1$  and  $W_2$  take on high values. From Fig. 7 one sees that for a prescribed value of stiffness  $c$ , one can find optimal values of  $\lambda$  and  $b$  with respect to index  $W_1$ . A considerable decrease of the values of both indices for parameter  $\lambda$  higher than some value is related to the system reaching the boundary of the stability region. Figure 8 shows that replacing the viscous damping coefficient of the motion of the piston inside the cylinder with dry friction does not have any qualitative effect on the relationships  $W_1(\lambda)$  and  $W_2(\lambda)$ . Analysing the plots in Fig. 9 one can conclude that in the system with buffers, for a prescribed  $b$ , the indices  $W_1$  and  $W_2$  increase with  $\lambda$  (within the stability range).

The time plot of the handle acceleration  $a_x(t)$  shown in Fig. 10 shows the effect of impacts of the handle against the buffer during the initial stage of the simulated work cycle. The buffers are active when the relative displacement  $w$  exceeds the value 0.03 [m]. The duration of this phase is relatively long since a small value of the parameter  $\lambda = 0.5 \cdot 10^4$  [N/ms] has been used. Figure 11 shows a similar plot obtained for  $\lambda = 2 \cdot 10^4$  [N/ms]. It is seen that the impact against

the handle is short and the acceleration values are lower. The figures also show the corresponding plots of relative displacements  $w(t)$ , which are substantially lower in the latter case.

#### REFERENCES

1. Z. BASISTA, *The influence of a vibration-insulated handle on the ergonomic comfort of a percussive tool* [in Polish], *Zeszyty Naukowe Politechniki Rzeszowskiej*, Nr 197, Mechanika 60, 19–26, Rzeszów 2002.
2. Z. BASISTA, M. KSIĄŻEK, *Estimation of comfort parameters of an active vibration isolation system of the handle of a percussive power tool*, Proceedings "INTER-NOISE'2004" Prague, August 22–25, "The 33<sup>rd</sup> International Congress and Exposition on Noise Control Engineering".
3. Z. BASISTA, *Computer analysis of an active vibration insulator in a man-tool-base system* [in Polish], *Czasopismo Techniczne*, Mechanika 5-M/2004, Kraków 2004, X Konferencja Naukowa "Wpływ wibracji na otoczenie", 26–37, Kraków 2004.
4. B.T. SHERIDAN, W. FERREL, *Man-machine systems*, The MIT Press, Cambridge 1974.
5. A. MODJTAHEDZADEH, R.A. HESS, *A model of driver steering control behavior for use in assessing vehicle handling qualities*, *Transactions of ASME, Journal of Dynamic Systems Measurement and Control*, **115**, 456–464, 1993.
6. S. RAKHEJA, J.Z. WU, R.G. DONG, A.W. SCHOPPER, *A comparison of biodynamic models of the human hand-arm system for applications to hand-held power tools*, *Journal of Sound and Vibration*, **249**, 1, 55–82, 2002.
7. V.I. BABITSKY, *Hand-held percussion machine as discrete non-linear converter*, *Journal of Sound and Vibration*, **214**, 1, 165–182, 1998.
8. E.V. GERTZ, *Dynamics of pneumatic systems of machines* [in Russian], *Masinstroenie*, Moskva 1985.

*Received June 13, 2005.*

---